Optics Communications 281 (2008) 4589–4597

Contents lists available at ScienceDirect

Optics Communications

journal homepage: www.elsevier.com/locate/optcom

Occlusion removal technique for improved recognition of partially occluded 3D objects in computational integral imaging

Dong-Hak Shin [a], Hoon Yoo [a,*], Chun-Wei Tan [a], Byung-Gook Lee [a], Joon-Jae Lee [b]

[a] Department of Visual Contents, Dongseo University, San69-1, Jurye2-Dong, Sasang-Gu, Busan 617-716, Republic of Korea
[b] Department of Game Mobile Contents, Keimyung University, 2139 Daemyung3-Dong, Nam-Gu, Daegu 705-701, Republic of Korea

ARTICLE INFO

Article history:
Received 5 December 2007
Received in revised form 11 April 2008
Accepted 4 June 2008

Keywords:
3D imaging
Integral imaging
Computational reconstruction
Occlusion removal

ABSTRACT

In this paper, we propose an occlusion removal technique for improved recognition of 3D objects that are partially occluded in computational integral imaging (CII). In the reconstruction process of a 3D object which is partially occluded by other objects, occlusion degrades the resolution of reconstructed 3D images and thus this affects negatively the recognition of a 3D object in CII. To overcome this problem, we introduce a method to eliminate occluding objects in elemental image array (EIA) and the proposed method is applied to 3D object recognition by use of CII. To our best knowledge, this is the first time to remove occlusion in CII. In our method, we apply the elemental image to sub-image (ES) transform to EIA obtained by a pickup process and those sub-images are employed for occlusion removal. After the transformation, we correlate those sub-images with a reference sub-image to locate occluding objects and then we eliminate the objects. The inverse ES transform provides a modified EIA. Actually, the modified EIA is considered to be an EIA without the object that occludes the object to be reconstructed. This can provide a substantial gain in terms of the image quality of 3D objects and in terms of recognition performance. To verify the usefulness of the proposed technique, some experimental results are carried out and the results are presented.

1. Introduction

Integral imaging is a promising technique for three-dimensional (3D) imaging. Integral imaging is able to work with the incoherent light and does not require the help of special viewing glasses [1–7]. From the proposal of integral imaging in 1908, it has raised a great attention to researchers because integral imaging is considered to be a promising technology to provide the observing images with the full parallax and the continuous viewing points. A general integral imaging system consists of two processes: pickup and reconstruction. In the pickup process, light rays emanating from 3D objects are captured by a lenslet array. The light rays passing through each lenslet are recorded by using a 2D image sensor such as the charged-coupled device (CCD). The captured images are considered to be a set (or array) of demagnified 2D images because each of them contains the different perspective information about the 3D objects. These demagnified 2D images are known as the elemental image array (EIA). Reconstruction of 3D objects is a reverse process of pickup by propagating the rays coming from EIA through the same lenslet array. The reconstruction of 3D objects can be done in two ways, either an optical way or a computational way.

For 3D visualization and recognition using InIm, computational integral imaging (CII) systems have been introduced [8–18]. A CII system is shown in Fig. 1a. It is composed of the optical pickup and the volumetric computational reconstruction (VCR) based on the pinhole-array model [10]. In optical pickup, 3D object is recorded as the EIA through a lenslet array. In the VCR process, the EIA is digitally processed by use of a computer where 3D images can be easily reconstructed at any reconstruction output plane without optical devices.

Even though VCR provides the simple reconstruction of 3D objects using only a computer, there are some problems to be solved including a poor visual quality by artifacts, high computation loads. In order to improve the visual quality in VCR, several methods are suggested. One is to use the moving array lenslet technique [12], in which the sampling rate of the EIA can be increased by the rapid moving of a lenslet array and the fast pickup of the EIA via time-multiplexing. However, this method has some difficulties. It may have a mismatch between the pickup lenslet array and the 2D image sensor caused by fast mechanical movement of the lenslet array. Also it requires the long multi-step pickup time to capture an EIA. Another method is to reconstruct resolution-enhanced 3D images using the intermediate-view reconstruction technique [15]. With this technique, intermediate elemental images can be digitally synthesized as many as required by using only a limited number of picked-up EIA and from which resolution-enhanced

* Corresponding author. Tel.: +82 51 320 1734.
E-mail address: hunie@dongseo.ac.kr (H. Yoo).

0030-4018/$ - see front matter © 2008 Elsevier B.V. All rights reserved.
doi:10.1016/j.optcom.2008.06.026

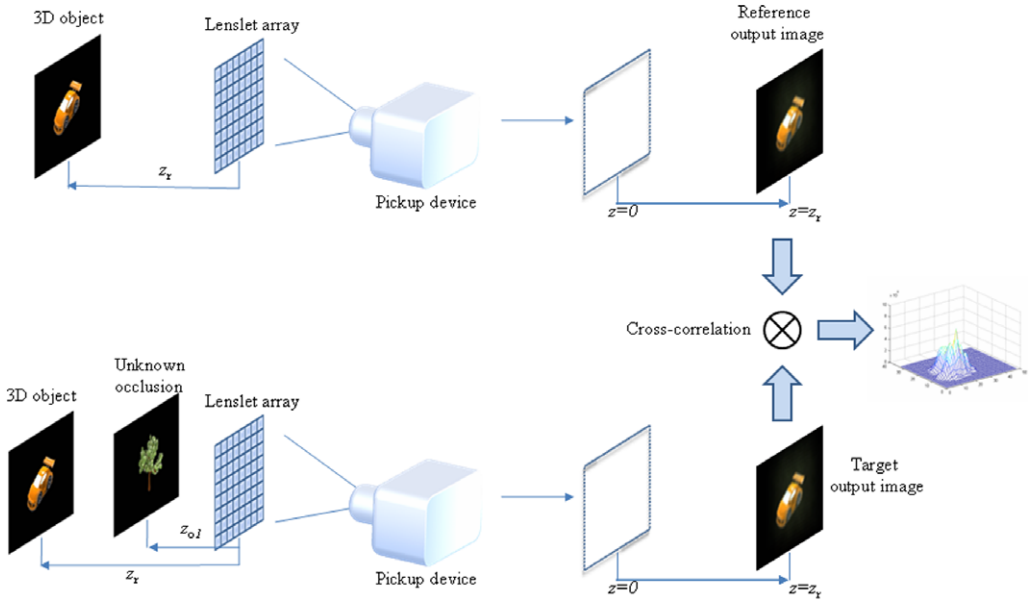

Fig. 1. Conventional CII system for partially occluded 3D object recognition: (a) reference CII system; (b) target CII system.

3D images can be reconstructed. Recently, another VCR method to reconstruct resolution-enhanced 3D images using an image interpolation technique has been proposed [16].

As a good application of CII, the most noticeable study is how to recognize a 3D object that is partially occluded in a given scene [13,14]. The principle to recognize a partially occluded object is to produce 3D volumetric reconstructed images and to correlate them with original 3D object [13–15]. Thus, the recognition performance is proportional to the quality of reconstructed 3D images in VCR. To do so, the previous improved VCR methods can be used. In partially occluded object recognition, however, the unknown occlusion makes the resolution of reconstructed images degraded seriously because it hides the 3D object to be recognized. This problem cannot be solved by helping any modification of VCR. Even if this is a main problem, there is no report to our best knowledge in CII. To enhance the recognition performance of CII, the reconstruction effect by occlusion should be considered.

In this paper, we propose an occlusion removal technique for improved recognition using CII. In the reconstruction of a partially occluded 3D object, unknown occlusion makes the resolution of reconstructed images degraded seriously. Therefore, the proposed technique introduces a technique to eliminate the unknown occlusion in the EIA and to reconstruct 3D images computationally. To eliminate occlusion, the input EIA is transformed into a sub-image array by the elemental image to sub-image (ES) transform and a central sub-image (CSI) is extracted for occlusion elimination. The correlation between each sub-image of the target object and the extracted CSI is performed. Through the correlation process, we select the effective sub-images and generate a modified EIA. Actually, the modified EIA is considered to be an EIA without the object that occludes the object to be reconstructed. This can provide a substantial gain in terms of the image quality of 3D objects and in terms of recognition performance. To verify the usefulness of the proposed technique, some experimental results are carried out and the results are presented.

2. Review of CII system for partially occluded 3D object recognition

The principle of partially occluded 3D object recognition using CII is that it is possible to obtain the reconstruction of the 3D plane image of interest. That is, we can reconstruct the plane image of the 3D object with reduced occlusion. The whole recognition system has two CII systems as shown in Fig. 1 [13]. One is the reference CII system and the other is the target CII system. Each system is composed of the pickup process and the VCR process.

In the reference CII system as depicted in Fig. 1a, a 3D reference object is captured by a lenslet array and a CCD camera. This pickup process produces an array of elemental images as a result. Here we call the array of elemental images as the reference EIA (elemental image array). Next the reference EIA is employed by VCR to reconstruct a plane image at the distance z_r where the 3D reference object is located. We call the plane image produced from the reference EIA as the reference template or template. The template is stored in a computer memory for pattern matching.

In the target CII system as shown in Fig. 1b, an object partially occluded by another object is recorded as another array of elemental images and this is called as the target EIA. Also, VCR produces a plane image from the target EIA. Here, the location of the two objects is unknown. This implies that VCR should produce lots of plane images along the z-direction to locate the exact position of the 3D reference object or the template.

The correlation process can be performed between the plane images and the template. Thus the argument of the maximum of correlation coefficient can be used for the location of the template.

3. Proposed technique for improved recognition of partially occluded 3D object

3.1. Description of CII system using the proposed technique

The principle of the proposed CII system using an occlusion removal technique is shown in Fig. 2. If our system is compared with the conventional CII system, there are two additional processes that are applied to the target EIA. The first process is to extract a CSI using the ES transform, which is a digital process to convert an EIA into a sub-image array. The second process is to generate a modified EIA where the unknown occlusion is removed by the proposed occlusion removal technique.

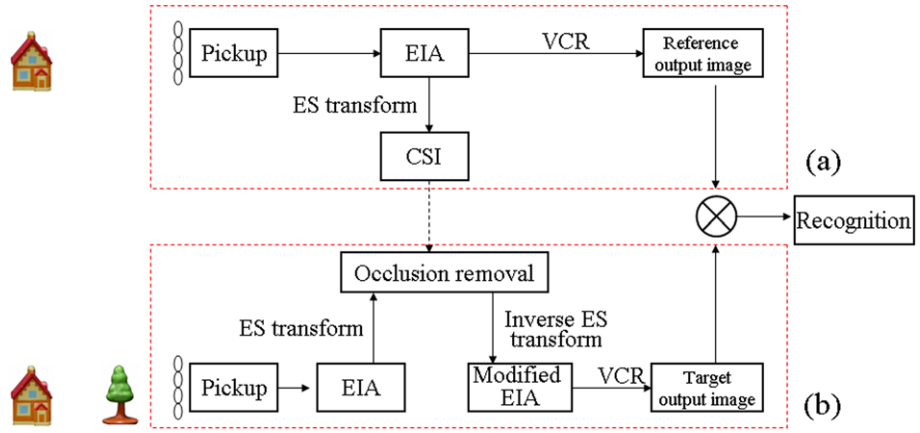

Fig. 2. Schematic diagram of the CII system using the occlusion removal technique: (a) reference CII system; (b) target CII system.

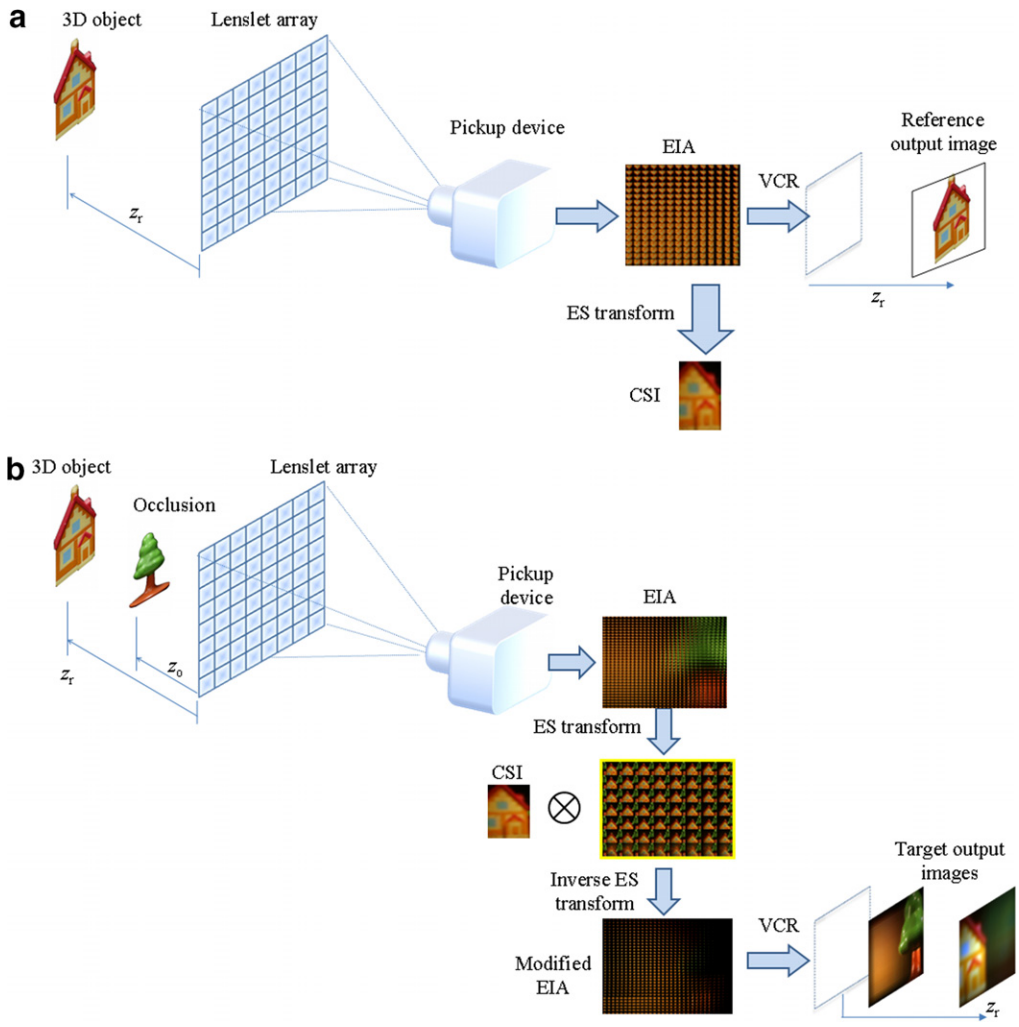

Fig. 3. Details of CII system using the proposed technique: (a) reference CII; (b) target CII.

3.2. Extraction of CSI in the reference CII

Fig. 3 illustrates the details of the proposed CII system. In the reference CII of Fig. 3a, it is commonly assumed that a 3D reference object is placed at a known distance. The template is obtained from the reference EIA using VCR. This process is the same as that of the conventional system. Here we extract the additional feature from the reference EIA for the occlusion removal. To do so, we use the ES transform as shown in Fig. 4. The principle of the ES transform is as follows. Suppose that all elemental images are represented as E with $s_x l_x \times s_y l_y$ pixels. Here s_x and s_y are the number of pixels for each elemental image and l_x and l_y are the number of elemental

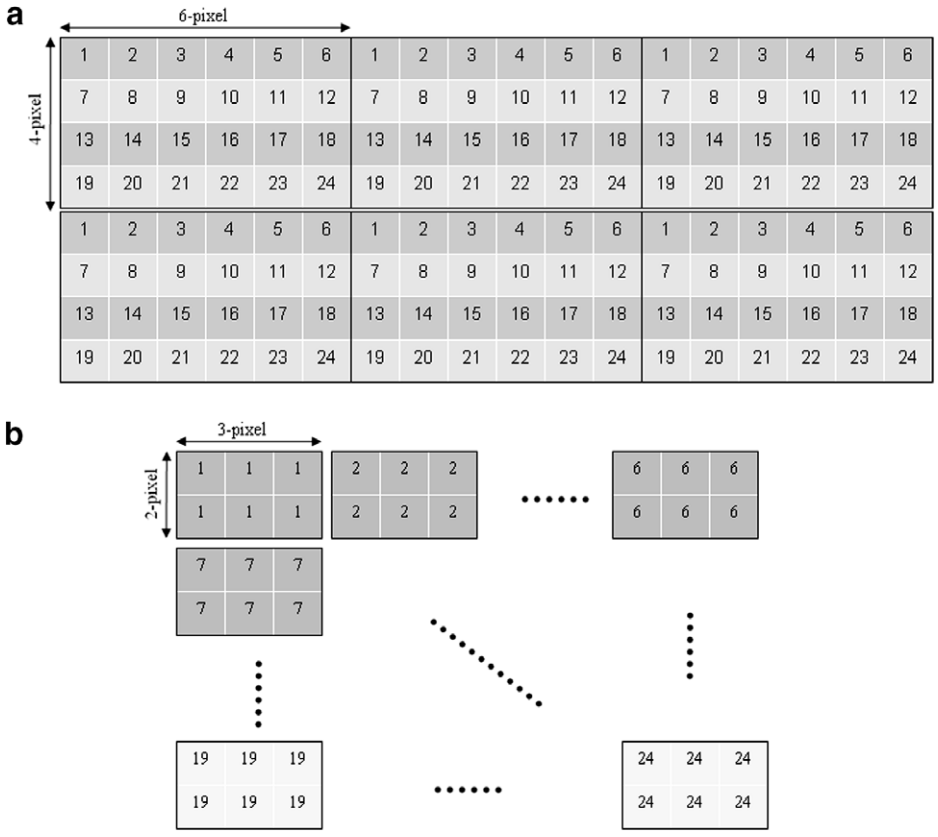

Fig. 4. Conceptual model of ES transform: (a) EIA; (b) sub-image array.

images in the x- and y-axis, respectively. Then a sub-image array is calculated by

$$S_{i,j}(m,n) = E_{m,n}(i,j) \tag{1}$$

where $i = 1,\ldots,s_x, j = 1,\ldots,s_y, m = 1,\ldots,l_x$ and $n = 1,\ldots,l_y$. This means that a sub-image is a set of pixels that are located at same position in each elemental image. For example, let us consider a 3×2 EIA and each elemental image consists of 6×4 pixels. After the ES transform using Eq. (1), the sub-image array becomes to be 6×4 sub-images whose size is 3×2, as shown in Fig. 4. This ES transform has been used in some applications [18,19].

After the ES transform, we have the sub-image array and can define the CSI (central sub-image) as

$$\mathrm{CSI} = S_{i=s_x/2,j=s_y/2} \tag{2}$$

And the CSI is used for a reference template for the proposed system. The CSI is a portion of the sub-image in the center of a sub-image array and its shape information is available because we already know the reference EIA exactly. In other words, it is possible to situate a 3D reference object at a known background. The proposed reference CII system uses a black background. This means that the pixel value of the background is zero whereas that of the 3D reference object is nonzero. Consequently, we can easily define the shape information of the CSI as

$$\alpha(i-i_0, j-j_0) = \begin{cases} 1, & \mathrm{CSI}(i,j) \neq 0, \\ 0, & \mathrm{CSI}(i,j) = 0. \end{cases} \tag{3}$$

Here, $i = i_0,\ldots,i_0+N-1$ and $j = j_0,\ldots,j_0+M-1$, where the location (i_0, j_0) is the coordinate of the upper-left corner of the smallest box that has the target object in the CSI and the size of box is (N, M). Also, we can extract the smallest box from the CSI and we can update the CSI with the smallest box. This updating process of the CSI is easily presented in the form

$$\mathrm{CSI}(i-i_0, j-j_0) = \mathrm{CSI}(i,j) \tag{4}$$

Here, $i = i_0,\ldots,i_0+N-1$ and $j = j_0,\ldots,j_0+M-1$. Largely, the updated CSI is smaller than the CSI of Eq. (2) and this improves the computation speed. Note that the CSI has a good feature that provides the robustness on the shifting effect of an object because it represents the center view of a 3D object. There are some examples in Fig. 5. According to the distance, the EIA is largely changed but the associated sub-image array is not changed. This robustness is very helpful for the recognition of objects.

3.3. Recognition in the target CII system

Now let us consider the proposed target CII system as shown in Fig. 3b. Let us assume that the unknown occluding object $O(x_o, y_o, z_o)$ and a target object are located at arbitrary distances z_o and z_r, respectively. Then these objects are picked-up by using a CCD camera as shown in Fig. 4b. This pickup process provides us a target EIA. And then the target EIA is transformed into a sub-image array. Each sub-image in the sub-image array is correlated with the CSI from the proposed reference CII system. This correlation process gives a set of correlation coefficients $C(r,c)$ and it can be written as

$$C(r,c) = \sum_{i=0}^{N-1}\sum_{j=0}^{M-1} \alpha(i,j)\mathrm{CSI}(i,j)S(r+i,c+j), \tag{5}$$

where $\alpha(i,j)$ is the shape information of the CSI, which is discussed in previous chapter. The value M and N denote the row and column size of the CSI, respectively. S denotes each sub-image. After correlation process of (5), we have a set of correlation coefficients. And then the arguments r_m and c_m of the maximum correlation coefficient $C_{\max}$ is chosen as the position information of the target object in each sub-image. Before moving on the next step, the value of $C_{\max}$ is compared with a threshold θ_{th}. If $C_{\max}$ is greater than the

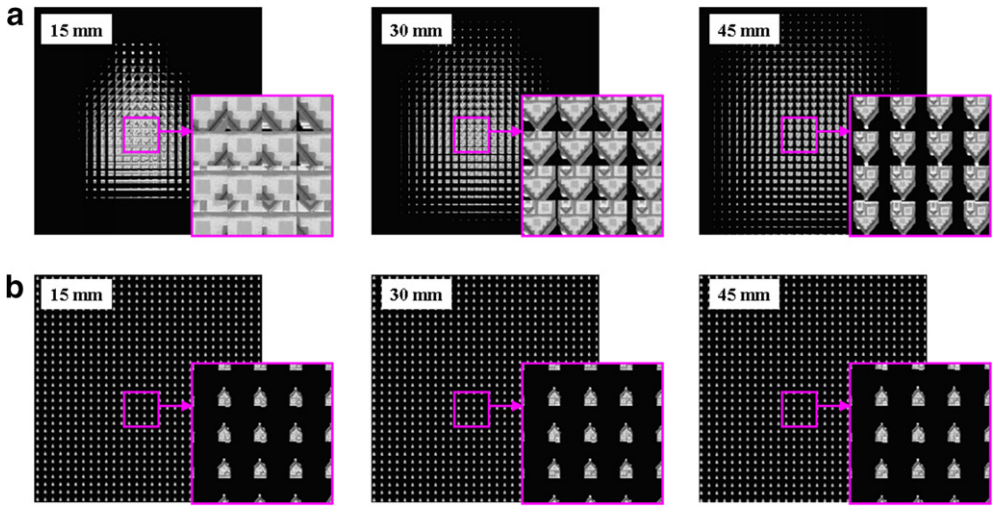

Fig. 5. Image characteristics according to the distance: (a) EIA; (b) sub-image array.

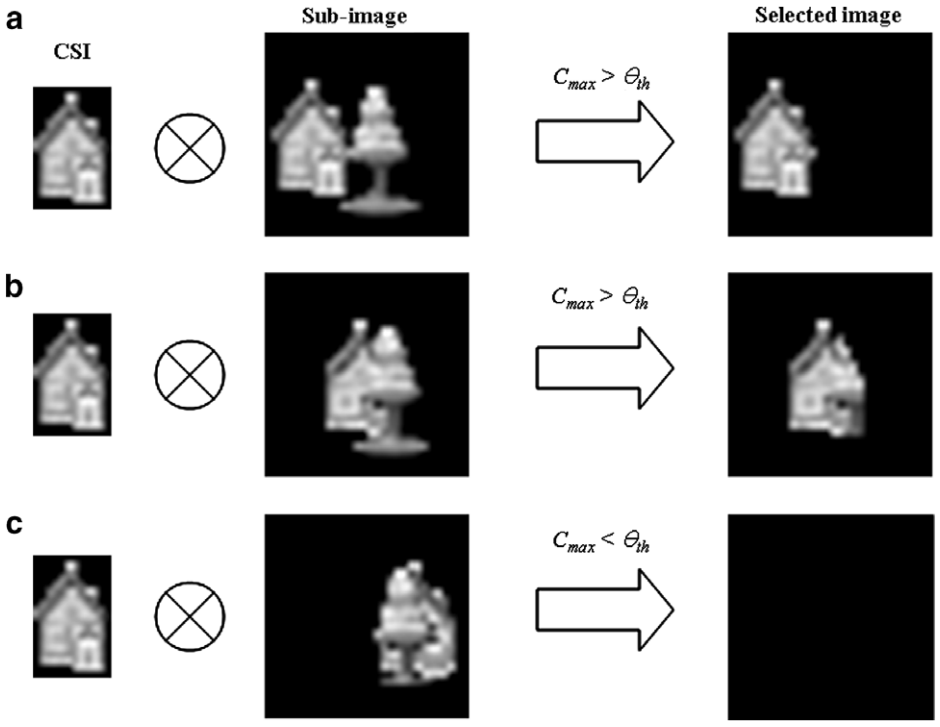

Fig. 6. Examples for sub-image selection. Here the operation $\otimes$ denotes the correlation process defined by Eq. (2).

threshold, the sub-image is modified; otherwise, the sub-image is set to be zero. Based on this, we can define a modified sub-image as

$$S_{\mathrm{mod}}(r_{\mathrm{m}}+i,c_{\mathrm{m}}+j)=\begin{cases} S(r_{\mathrm{m}}+i,c_{\mathrm{m}}+j) & \alpha(i,j)=1 \text{ and } C_{\max}\geqslant\theta_{\mathrm{th}}, \\ 0 & \text{otherwise.}\end{cases} \tag{6}$$

To facilitate understanding of the proposed correlation process, we illustrate some examples in Fig. 6. Here we show three cases of correlation between the CSI and sub-images. Fig. 6a shows the correlation process between the CSI and a sub-image in case that the target object is not occluded by another object in the sub-image. Referring to (5) and (6), we have the visual results as depicted in Fig. 6a. Fig. 6b shows the situation that the target object is slightly occluded by the unknown occluding object. The case is that the correlation peak is larger than the threshold θ_{th}, because the occluded area is small. In this case, the process defined in Eq. (6) is still valid. Its visual result in Fig. 6b indicates that the unknown occluding object is partially removed. Fig. 6c shows that the target object is fully hidden by unknown occlusion. Thus the correlation peak of this case is considered to be less than the threshold θ_{th}. And thus the sub-image is discarded entirely. According to the results of Fig. 6, it is seen that removal of occlusion depends on the threshold θ_{th}. As θ_{th} increases, the number of sub-images in the sub-image array decreases and then some information of the target object may be lost. Therefore, there is an optimal threshold for 3D image reconstruction and this can be estimated by repeating the computational process for different values.

For all sub-images, the correlation process and modification based on Eq. (6) can be performed. Actually, these processes give us a modified sub-image array. The sub-image array is transformed back to an EIA by the inverse ES transform. The EIA is a modified version of the original EIA.

By using the newly modified EIA, plane images are reconstructed by using VCR and are denoted by $R(x, y, z)$ at the distance z. The correlation process for object recognition can be performed between these plane images and the template $T(x, y, z_r)$ from the reference CII. Accordingly, we can obtain correlation results using the following correlation operation as given by

$$\mathrm{Corr}(x, y, z) = R(x, y, z) \otimes T(x, y, z_r) \tag{7}$$

The correlation process is repeated for all plane images by varying the distance z. Thus the argument of the maximum of correlation coefficient can be used for the location of the template. In fact, the image quality of the plane images from the occlusion-removed EIA can superior to that of the plane images without occlusion removing. Therefore, a recognition process using our technique can provide a substantial gain in terms of image quality.

4. Experiments and results

To show the usefulness and objective evaluation of the proposed technique, we carry out computational experiments on 3D objects. The experimental structure is shown in Fig. 7. The target object to be recognized is the image 'house'. This is located at z_r = 48 mm. The 'tree' image is used as the unknown occluding object located at z_o = 12 mm from the lenslet array.

First, the target object is captured through a lenslet array in the reference CII system as shown in Fig. 4a. Here the lenslet array consists of 30 × 30 lenslets, and the lenslet diameter is 1.08 mm. With the lenslet array, we obtained the EIA having the resolution of 900 × 900 pixels. The captured EIA was transformed into the associated sub-image array and a CSI was extracted as described in Eq. (4). And the shape information of Eq. (3) was extracted using the selected CSI. Fig. 8a and b shows the EIA and the sub-image array of the target object, respectively. In the sub-image array, the CSI defined in this experiment is shown in Fig. 8c.

In the target CII system as shown in Fig. 3b, the target EIA including the target object 'house' and the occluding object 'tree' was captured. The captured target EIA is shown in Fig. 9a. The EIA was transformed into the associated sub-image array using Eq. (1). Fig. 9b shows the result of the sub-image array transformed by the ES transform. Then, each of the sub-images was correlated with the CSI and its shape information by using Eq. (5). Based on the local correlation rule, as it is explained in Fig. 6, the area that are well matched with the template for each sub-image is extracted to form the new sub-image array as shown in Fig. 9c when θ_{th} = 0.95. This newly generated sub-image array is transformed back into the modified EIA by means of the inverse ES transform as shown in Fig. 9d.

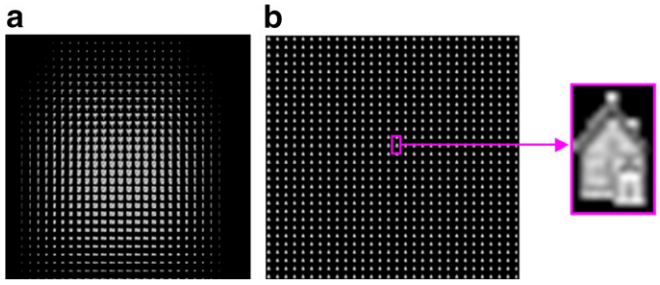

Fig. 8. (a) EIA of 3D object; (b) sub-image array; (c) CSI.

By using this newly generated EIA, two plane images were reconstructed at 12 mm and 48 mm by using VCR technique, respectively. Fig. 10a shows the original image of the unknown occlusion and Fig. 10b and c show the reconstructed images of the conventional CII system and the proposed CII system using the occlusion removal technique, respectively. Here we can see that the 'tree' occlusion is largely removed in the proposed method. This shows that the proposed technique removes the occlusion effectively. On the other hand, Fig. 11 shows the reconstructed images of the target 3D object at the distance of 48 mm. In the conventional system, the 'house' image shown in Fig. 11b is not clear and it has low contrast because of the blurring effect caused by the unknown occlusion. This is more clearly seen when the reconstructed images are compared with the original image as shown in Fig. 11a. However, we can see that the high contrast image reconstructed from the CII system using the proposed technique is obtained as shown in Fig. 11c. This may improve the correlation performance.

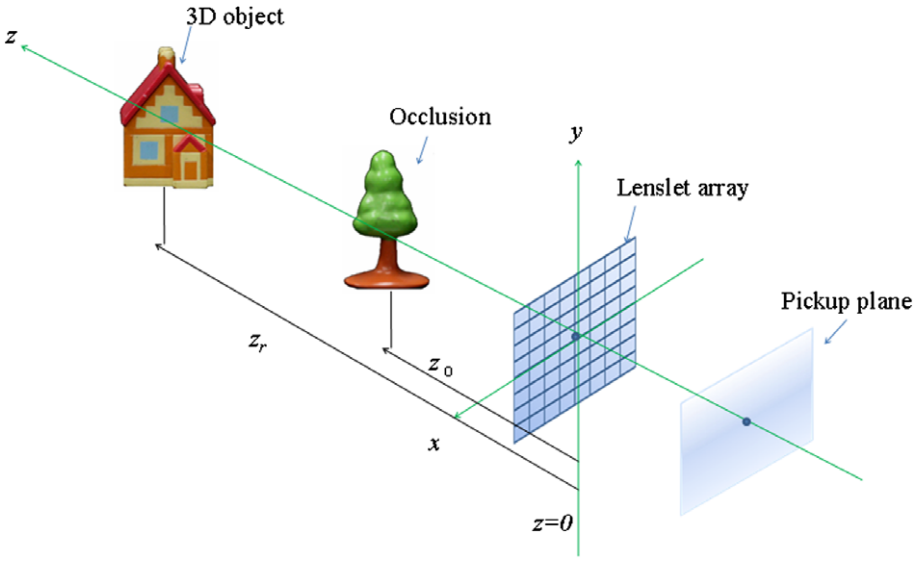

Fig. 7. Experiment structure.

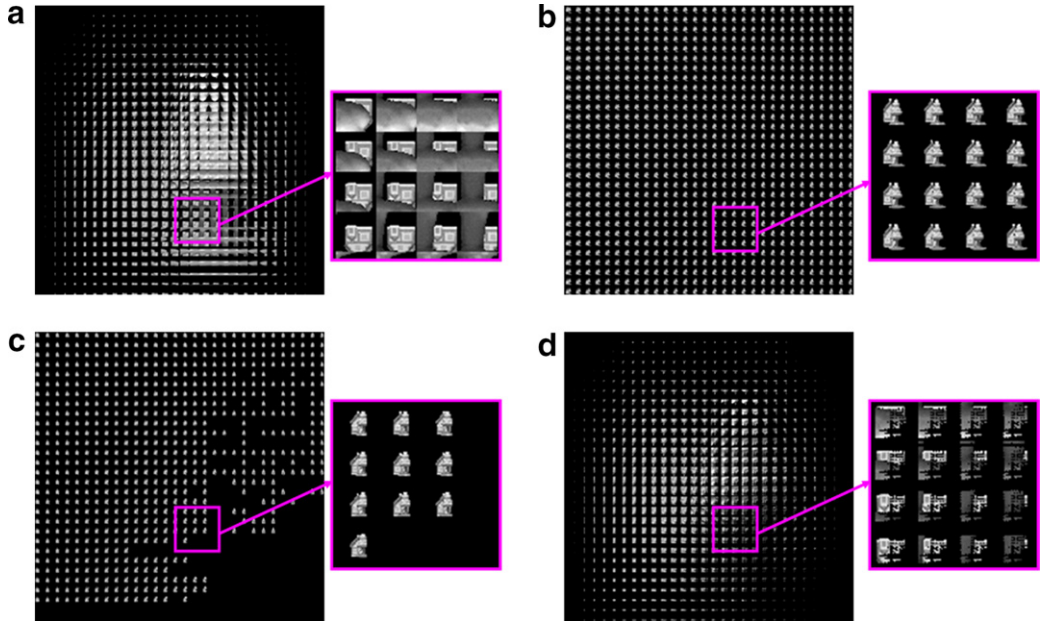

Fig. 9. (a) EIA of target objects; (b) sub-image array of target objects; (c) modified sub-image array; (d) modified EIA.

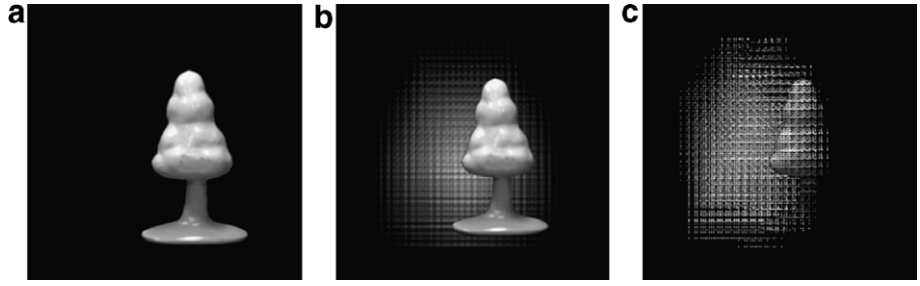

Fig. 10. Reconstructed images of the unknown occlusion when $z = 12$ mm and $\theta_{th} = 0.95$. (a) Original image; (b) conventional CII system; (C) CII system using the proposed technique.

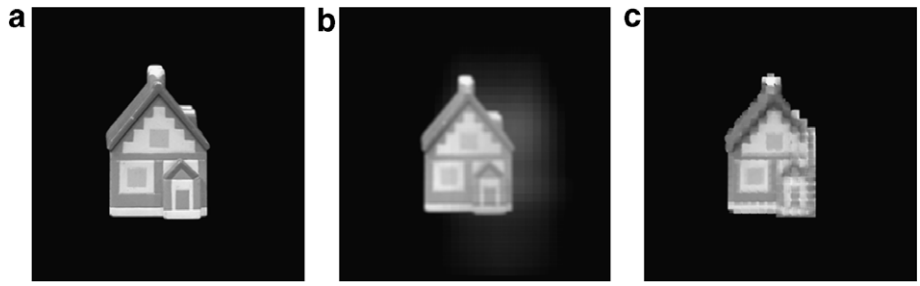

Fig. 11. Reconstructed images of the 3D object when $z = 48$ mm and $\theta_{th} = 0.95$. (a) Original image; (b) Conventional CII system; (c) CII system using the proposed technique.

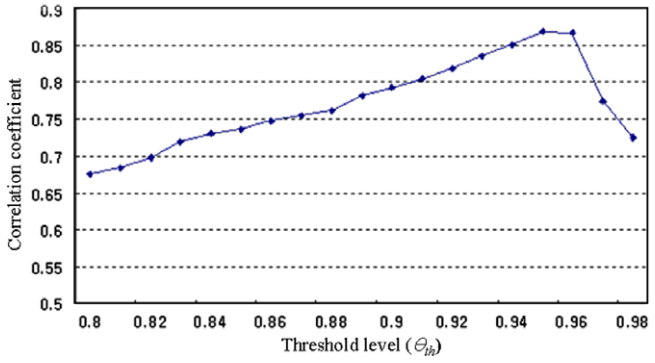

Fig. 12. Correlation coefficient according to the threshold level.

To show the correlation performance of the proposed CII system, we carried out the correlation between the original 'house' image and target plane images of 'house'. Target plane image depends on the selection of the effective sub-image in the target CII system. The level of a correlation peak for selecting the effective sub-images is an important parameter in this experiment. The correlation coefficients are compared with the threshold θ_{th}. Fig. 12 shows the correlation coefficients according to the threshold level. The best coefficient is approximately 0.87 when the threshold level is 0.95. The correlation coefficient is 0.61 in the conventional system. This result shows that the proposed method improves the correlation performance by 42%.

Under the same conditions, we carried out the additional experiments for the three test image set as shown in Fig. 13. To objec-

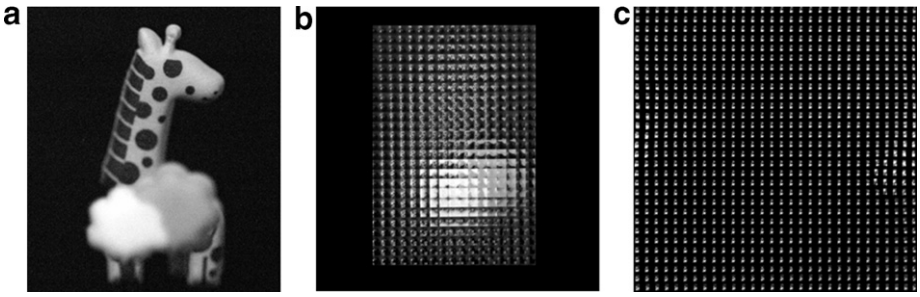

Fig. 13. (a) 3D objects for optical pickup; (b) EIA; (c) sub-image array.

Table 1
PSNR results for the four test image sets

Image set	1	2	3	4
Occlusion and object		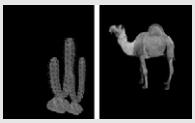		
Conventional method	21.38	23.88	22.67	18.22
Proposed method	29.29 (θ_{th} = 0.95)	24.49 (θ_{th} = 0.46)	24.91 (θ_{th} = 0.64)	24.34 (θ_{th} = 0.64)

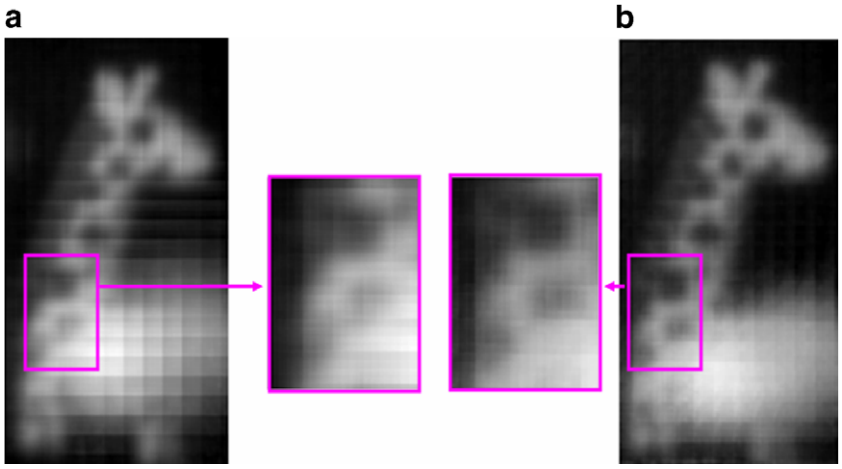

Fig. 14. Images reconstructed from EIA picked-up by an optical device. (a) Conventional system; (b) proposed system.

tively evaluate our experiments we also calculated the PSNRs for all test image set. PSNR is defined as

$$\mathrm{PSNR}(I_o, I_r) = 10\log_{10}\left(\frac{255^2}{MSE(I_o, I_r)}\right) \tag{8}$$

where I_o is an original image; and I_r is the reconstructed image from VCR process. And mean squared error (MSE) is given by

$$\mathrm{MSE} = \frac{1}{XY}\sum_{x=0}^{X-1}\sum_{y=1}^{Y-1}[I_o(x,y) - I_r(x,y)]^2 \tag{9}$$

where x and y are the pixel coordinates of images having $X \times Y$ pixels.

The PSNR results for test image sets are shown in Table 1. Our best results were calculated under the corresponding optimal threshold θ_{th} for each test set. From results of Table 1, it is revealed that the visual quality of images reconstructed from our method is better that that from conventional method. We obtained the improvement of average 4.22 dB in PSNR from these experiments.

Next, another experiment using an EIA of real 3D objects is carried out. The real 3D objects, as shown in Fig. 13a, are composed of two toys, 'trees' and 'giraffe'. The 'trees' and 'giraffe' objects are longitudinally located at $z = 12$ mm and $z = 24$ mm, respectively. The lenslet array of 25×17 lenslets is located at $z = 0$ mm. Each lenslet size is 1.08 mm and each elemental image is composed of 30×30 pixels. The captured EIA and the sub-image array are shown in Fig. 13b and c, respectively. Fig. 14 shows the reconstructed images at $z = 24$ mm for the both conventional system and the proposed system, respectively. It must be noted here that there is an improvement of visual quality between two reconstructed images. In the result of the conventional method of Fig. 14a, we can see the intensity irregularities with a grid structure cased by the square-shaped mapping of EIA. However, the proposed occlusion removal technique provides a substantial gain in terms of visual quality, as shown in Fig. 14b. This is due to eliminating occlusion by the proposed technique.

5. Conclusions

In this paper, we have proposed an occlusion removal technique for improved recognition of 3D objects that are occluded partially in CII. We have introduced a technique to eliminate occluding

objects in elemental image array and the proposed technique is applied to 3D object recognition by use of CII. To our best knowledge, this is the first time to remove occlusion in CII. In our proposed technique, we employed the ES transform to obtain an efficient occlusion removal. And then we proposed a correlate process to determine occluding pixels. This produces a modified EIA and it is considered to be an EIA without occluding objects that occlude the object to be reconstructed. This can provide a substantial gain in terms of the image quality of 3D objects and in terms of recognition performance. To obtain more improvement, we can combine the proposed technique with the previous improved VCR method. To show the usefulness of the proposed technique, we represented some experiments and demonstrated the improvement of recognition performance. Therefore, we expect that the proposed technique will aid to improve the performance of recognition systems using CII.

References

[1] G. Lippmann, C.R. Acad. Sci. 146 (1908) 446.
[2] F. Okano, H. Hoshino, J. Arai, M. Yamada, I. Yuyama, in: B. Javidi, F. Okano (Eds.), Three-Dimensional, Television, Video and Display Technology, Springer Verlag, Berlin, Heidelberg, NY, 2002, p. 101.
[3] A. Stern, B. Javidi, Proc. IEEE 94 (2006) 591.
[4] B. Lee, S.Y. Jung, S.-W. Min, J.-H. Park, Opt. Lett. 26 (2001) 1481.
[5] J.-S. Jang, B. Javidi, Opt. Lett. 27 (2002) 324.
[6] M. Martínez-Corral, B. Javidi, R. Martínez-Cuenca, G. Saavedra, J. Opt. Soc. Am. A 22 (2005) 597.
[7] D.-H. Shin, B. Lee, E.-S. Kim, Appl. Opt. 45 (2006) 7375.
[8] H. Arimoto, B. Javidi, Opt. Lett. 26 (2001) 157.
[9] Y. Frauel, B. Javidi, Appl. Opt. 41 (2002) 5488.
[10] S.-H. Hong, J.-S. Jang, B. Javidi, Opt. Express 12 (2004) 483.
[11] D.-H. Shin, E.-S. Kim, B. Lee, Jpn. J. Appl. Phys. 44 (2005) 8016.
[12] S.-H. Hong, B. Javidi, Opt. Express 12 (2004) 4579.
[13] B. Javidi, R. Ponce-Díaz, S.-H. Hong, Opt. Lett. 31 (2006) 1106.
[14] S.-H. Hong, B. Javidi, Opt. Express 14 (2006) 12085.
[15] J.S. Park, D.C. Hwang, D.H. Shin, E.S. Kim, Opt. Comm. 26 (2007) 72.
[16] D.-H. Shin, H. Yoo, Opt. Express 15 (2007) 12039.
[17] H. Yoo, D.-H. Shin, Opt. Express 15 (2007) 14107.
[18] J.-H. Park, J. Kim, B. Lee, Opt. Express 13 (2005) 5116.
[19] C. Wu, A. Aggoun, M. McCormick, S.Y. Kung, in: A.J. Woods, J.O. Merritt, S.A. Benton and M.T. Bolas (Eds.), Stereoscopic Displays and Virtual Reality Systems IX, Proc. SPIE 4660, 2002, 135.